Accuracy in evaluating heat transfer coefficient by RANS CFD simulations in a rectangular channel with high aspect ratio – Part 1: benchmark on a channel with plane walls

Maria CORTI, Pasqualino GRAMAZIO, Damiano FUSTINONI, Luigi VITALI and Alfonso NIRO*

Politecnico di Milano, Department of Energy
via Lambruschini 4, 20156 Milano, Italy

* Corresponding author e-mail: alfonso.niro@polimi.it

Abstract. Computational Fluid-Dynamics (CFD) simulations are widely used for designing components and devices for heat transfer enhancement, and to this end the Reynolds Averaged Navier-Stokes (RANS) equations are often chosen, as they are computationally efficient. In this paper, several numerical simulations have been carried out on convective heat transfer of an air flow through a rectangular channel of 1:10 aspect ratio, 120 mm wide, 840 mm long. Numerical results have been compared to analytical values and experimental data. The configuration of the described numerical model will be used as starting point for detailed investigations of fluid-dynamic and thermal performances of ribbed channels in further analysis.

Key Words: *forced convection, heat exchanger, rectangular channel, flat surfaces, experimental tests, CFD validation, RANS*

1. Introduction

Heat transfer enhancement in air forced convection is a contemporary technological issue, despite its decades of life. Especially associated to forced convection inside rectangular channels with various ribbed surfaces, it sees a wide range of applicability in engineering applications [1,2]. A cutting-edge solution is working with ribbed high aspect ratio channels at low Reynolds flow regimes. Channel with high aspect ratio, in addition to fulfil the industrial interest for narrow channels, ensures a wide central area undisturbed by edge losses that can be dedicated to heat transfer. At the ThermALab laboratory at Politecnico di Milano, authors have been and are currently involved in experimental analysis on fluid-dynamics and heat transfer characteristics of forced convection inside a channel with an aspect ratio of 1:10 [3-6]. To complement the experimental campaign with a CFD model, this work is carried out. It will be followed by an analysis regarding the accuracy in evaluating the global heat transfer coefficient by RANS CFD simulations in a high aspect ratio channel with and without ribs. As reported in [7], an appropriate tool is the use of finite volume CFD code. Knowing problems about the computational effort required to solve Navier-Stokes equations, with the present work authors are looking for a CFD model based on RANS that can be used as a starting point for future studies. In this paper, results on velocity profiles, pressure drops, and convective heat transfer coefficient are

presented along with a discussion on the comparison between analytical, experimental, and numerical data.

2. Problem configuration and set-up

2.1. Experimental set-up
The experimental set-up is described in detail in [3], briefly it consists in a rectangular channel of 1:10 aspect ratio. The main geometric parameters of the section dedicated to measurements, are summarized in Table 1. In this paper, all the walls of the channel are flat. The channel used in the experimental set-up operates with lower and upper walls maintained at fixed temperature, while side walls are adiabatic. The air flows at Reynolds numbers ranging from 700 to 8000.

2.2. Numerical procedure
Numerical simulations have been carried out using the software Ansys Fluent 19.1 based on finite volume method. The solution domain is a 3D channel with a rectangular cross section as described previously (Figure 1). The working fluid is air, incompressible, with constant specific heat coefficient.
To obtain a grid independent solution, a sensitivity analysis has been carried out. Since it is a three-dimensional case, given the three directions x, y, z where x is the direction of the channel width, y the direction of the channel height and z the streamwise direction, a sensitivity analysis has been carried out for each dimension.
Working at different Reynolds numbers [3-4], different flow regimes (laminar or turbulent) are considered so grids have been constructed respecting the needs of each case analysed.
Per example for laminar Reynolds, the number of elements for the whole channel has been around $5 \cdot 10^6$. For turbulent flow with Reynolds higher than 2000 up to 7500, the number of elements for the whole channel has been ranging from $6 \cdot 10^6$ to $40 \cdot 10^6$ ensuring a $y^+ = 1$ at the wall to solve the laminar sublayer.

2.3. Boundary conditions
Since the flow in the experimental set-up, at the inlet of the measurement section, can be considered hydrodynamically fully developed, this condition is required at the inlet of the present computational domain. For this purpose, some preliminary CFD simulations have been carried out. Considering an adiabatic channel with the same rectangular cross section, with plane walls and enough long in the streamwise direction to guarantee the hydrodynamic development both in laminar and turbulent case (for laminar flow regime: $x_{fd,h} \geq 0.05 ReD_h$, for turbulent flow regime: $x_{fd,h} \geq 10D_h$), it has been used to allow the full development of the airflow. The velocity profile (its three components), and, if needed, the corresponding turbulence parameters (Turbulent Kinetic Energy, k $[m^2/s^2]$ and Specific Dissipation Rate, ω $[1/s]$) obtained at the outlet of this preliminary channel have been used as inlet condition for the analysed cases.
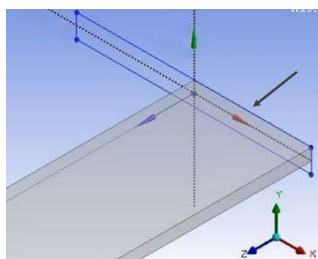

Figure 1. 3D domain.

Table 1. Main channel parameters.

Main channel parameters	
Channel height, 2b	12.0 mm
Channel width, 2a	120.0 mm
Channel length, L	840.0 mm
Hydraulic diameter, D_h	21.82 mm

2.3.1. Preliminary analysis on thermal boundary conditions

A preliminary analysis on thermal boundary conditions has been necessary for finding the most suitable configuration for boundary conditions in the CFD model.

For this reason, a simple case has been studied: a rectangular channel with plane walls and Reynolds number of 1083 has been modelled with CFD.

Boundary conditions of this preliminary case are summarized as follows:

- Inlet: velocity inlet (fully developed velocity profile, previously generated) based on the selected Reynolds number, in this case Re=1083. The working fluid is air, enters the channel at uniform temperature, $T_{in} = 296$ K.
- Outlet: pressure outlet $P_{out} = 0$ Pa.
- Walls: no-slip velocity condition is applied for all the walls, and the thermal condition has been benchmarked.

Coupled algorithm is used for pressure-velocity coupling. The presented laminar flow has been solved with Laminar model. Computational time has been restrained, 4-5 hours per each single simulation using 15 cores Intel(R) Xeon(R) Gold 6148 CPU @ 2.40GHz. Laminar simulations stop at the level-out point of the continuity residual.

The outlet velocity profile obtained numerically has been compared to the analytical velocity profile for a rectangular channel [8] obtaining the expected accurate prediction. This comparison can be graphically seen in Figure 2. Since the case considered is a fully developed velocity profile in a rectangular duct, the equation used for the comparison is the following, equation (1). Notice that n and m are dimensionless coefficients proposed by Purday [8] to reduce the complexity of the equation of the fully developed velocity profile for rectangular ducts. According to that, since the aspect ratio (named α* in the considered equations) is equal to 0.1, values of n=2 and m=13.6 have been used.

$$u_{\mathrm{m}} = -\frac{16}{\pi^3}\left(\frac{dP}{dw}\right)\frac{a^2}{\mu}\sum_{n=1,3,\ldots}^{\infty}\frac{(-1)^{(n-1/2)}}{n^3}\left(1 - \frac{\cosh(n\pi y/2a)}{\cosh(n\pi b/2a)}\right)\cos\left(\frac{n\pi x}{2a}\right) \tag{1}$$

$$u_{\mathrm{m}} = -\frac{1}{3}\left(\frac{dP}{dw}\right)\frac{a^2}{\mu}\left[1 - \frac{192}{\pi^5}\left(\frac{a}{b}\right)\sum_{n=1,3,\ldots}^{\infty}\frac{1}{n^5}\tanh\left(\frac{n\pi b}{2a}\right)\right] \tag{2}$$

$$\frac{u_{\mathrm{max}}}{u_{\mathrm{m}}} = \left(\frac{m+1}{m}\right)\left(\frac{n+1}{n}\right) \tag{3}$$
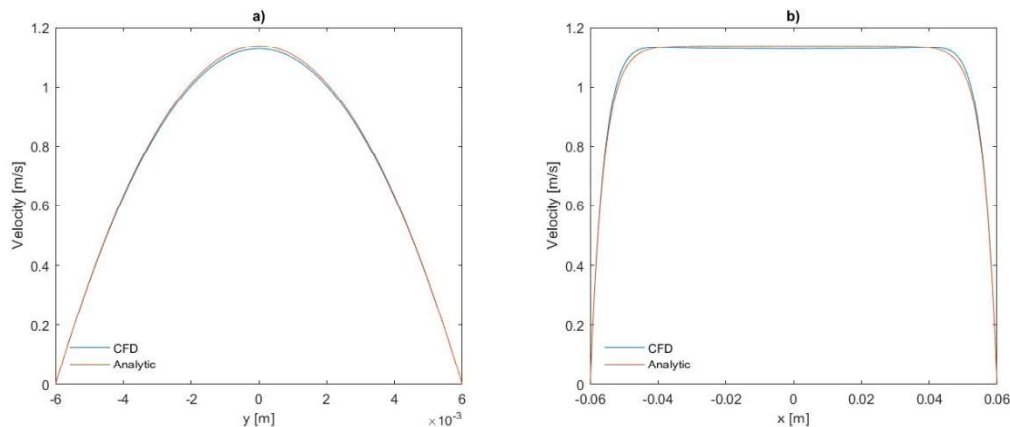
Figure 2. Comparison between numerical and analytic profiles of dimensionless velocity in laminar flow regime at Re=1083. The velocity profile is represented (a) versus y and (b) versus x, respectively height and spanwise directions.

Subsequently, Darcy friction factor obtained from numerical results on the channel at Re=1083 has been compared with the value obtained analytically for a laminar flow, fully developed, inside a rectangular channel adopting equation (4) proposed by Shah and London [9], written below.
Table 2 shows this comparison, it's clear the accurate agreement between the two values considered.

$$f_{Darcy} = 96 \left(1 - 1.3553\alpha^* + 1.9467(\alpha^{*2}) - 1.7012(\alpha^{*3}) + 0.9564(\alpha^{*4}) - 0.2537(\alpha^{*5}) \right) / Re \quad (4)$$

At this point, considering heat transfer, some boundary conditions for walls have been tested to find the most suitable boundary condition for the studied channel to apply to the CFD model:
- case 1: upper and lower walls heated at constant temperature, imposing $T_w = 323.15K$, while lateral walls considered adiabatic, imposing $\dot{q} = 0\,W/m^2$
- case 2: upper, lower, and lateral walls heated at constant temperature, imposing T_w
- case 3: upper and lower walls heated at constant temperature, imposing T_w, while at lateral walls a boundary condition of the third type has been considered, imposing a convective heat transfer coefficient $h = 4.5\,W/m^2/K$ and a free stream temperature $T_\infty = 293K$
- case 4: upper, lower, and lateral walls heated at constant temperature, imposing $\dot{q}$.

The thermal boundary condition that fits better the experimental set-up is case 2, in fact, the choice of setting all the walls of the channel as heated walls while in the experimental setup lateral walls are considered adiabatic returns an error on the experimental values of the Nusselt number lower than 7-10%. Probably, given the high aspect ratio of the considered channel, in the experimental measurements, the tiny lateral walls tend to be heated from the upper and the lower walls due to conduction phenomena. To better understand why this approximation can be accepted is recommended to deepen the working conditions of the experimental setup, accurately described in [3]. This approximation applied to the numerical boundary conditions to better represent the experimental configuration is applied to all the following CFD simulations carried out.

2.3.2. Adopted boundary conditions
- Inlet: velocity inlet (fully developed velocity profile, previously generated) basing on the selected Reynolds number. The working fluid is air, enters the channel at uniform temperature, $T_{in} = 296$ K. The fluid flow is not thermally developed yet, so the temperature will develop inside the considered channel.
- Outlet: pressure outlet $P_{out} = 0Pa$.
- Wall: no-slip velocity condition is applied for all the walls, moreover the walls (lower, upper, and lateral) are heated at constant temperature, imposing $T_w = 323.15K$.
- Symmetry: since it can be considered a symmetric case in the x-direction and in the y-direction (spanwise), symmetry has been applied at the wall identified from the centrelines to save computational time.

2.4. Solver setting and model
The Semi-Implicit Method for Pressure Linked Equation (SIMPLE) algorithm is used for pressure-velocity coupling. The presented turbulent flows have been solved with RANS, particularly choosing the k-ω-SST model. It uses as default the Enhanced Wall Treatment, a wall function for the near-wall region i.e., viscous sublayer, buffer region and fully turbulent outer region.

Table 2. Comparison between numerical and analytic value of Darcy friction factor in fully developed flow inside rectangular channel at Re=1083.

Re	f_{Darcy}	f_{CFD}	e%
1083	0.07821	0.07823	0.03%

Computational time has been considerable with respect to laminar case; up to 60 hours of calculations were needed per each single case for turbulent flows using 15-30 cores Intel(R) Xeon(R) Gold 6148 CPU @ 2.40GHz. RANS simulations stop when the continuity residual is lower than $1 \cdot 10^{-6}$.

3. Validation of results

The numbers of Reynolds considered in this study have been precisely: 2168, 3249, 5399 and 7552. Per each Reynolds number a CFD simulation has been carried out analysing in particular the agreement of numerical results with analytical and experimental data. The experimental data considered can be found in [3], in which values of the average Nusselt number inside flat rectangular channel for the range of Reynolds tested experimentally are presented in Figure 3, please refer to the case reported as "Flat T" in the legend.

3.1. Pressure drops

Friction factors obtained from pressure drops deriving from numerical results through equation (5) have been compared with analytical values.

$$f_{Darcy} = \left(\Delta P_0 / 0.5 \rho u^2\right)\left(D_h / L\right) \tag{5}$$

For turbulent flow in a rectangular channel, the correlations used have been the one of Kakac-Shah [8], based on Techo correlation [10] and adjusted for rectangular ducts, and PKN correlation [11-13]. Kakac-Shah correlation, equation (6), is valid for $0 \leq \alpha^* \leq 1$ and, preferentially, $5000 \leq \text{Re} \leq 10^7$, it has the following structure:

$$f = \left(1.0875 - 0.1125 \alpha^*\right) f_{Techo} \tag{6}$$

PKN correlation is valid for all arbitrarily large Reynolds number as reported in [8]. Errors between those values are shown in Table 3.

For Reynolds number higher than 5000 the agreement with analytical results is quite good, meaning errors lower than 12%, while for Reynolds number lower than 5000 the agreement is lower meaning errors up to 27%.

3.2. Convective heat transfer coefficient

Bulk temperature T_b and heat flux $\dot{q}$ have been calculated as mean section variables, from which can be calculated the local convective heat transfer coefficient $h_z = \dot{q}_z / (T_w - T_b)$ and consequently the related Nusselt number at any location along the channel $\text{Nu}_z = h_z D / k$. This Nusselt number obtained is considered a local Nusselt number at a specified location, in this case the section of interest is the outlet of the channel.

From computational results, since the flow is hydrodynamically and thermally developed (for turbulent flow regime a $x_{fd,th} \geq 10 D_h$ can be assumed [14]), also a mean Nusselt number can be calculated from an energy balance.

The mean convective heat transfer coefficient is computed as $h_m = \dot{m} c_p (T_{out} - T_{in}) / A / \Delta T_{m,ln}$ and the associated Nusselt number is $\text{Nu}_m = h_m D / k$.

To compare Nusselt numbers obtained from CFD results with Nusselt number obtained by analytical correlation, correlation by Gnielinski [14] for forced convection in turbulent pipe flow has been used, considering the effect related to the entrance to compare also the mean Nusselt number.

For low Reynolds numbers, errors on Nusselt number have been considerable, while good agreement has been obtained for Reynolds numbers higher than 5000, obtaining errors lower than 15-10%.

Values of Nusselt number calculated analytically and from CFD results are presented in Table 4, per each value the associated error is shown, as the error with respect to Nusselt numbers measured experimentally.

3.2.1. Analysis for the choice of RANS model for low Reynolds numbers

Basing on these results, some RANS turbulence models have been investigated to find more reliable results even for low Reynolds number. Considering Reynolds 3249, the following RANS models have been tested:

- k-ω-SST with a mesh that ensures $y^+=1$
- k-ω-SST with a mesh that ensures $y^+=0.8$
- k-ω-SST with a mesh that ensures $y^+=0.2$
- k-ω-SST with a mesh that ensures $y^+=1$ and Low Reynolds option
- k-ε RNG with a mesh that ensures $y^+=0.8$
- k-ε Realizable a mesh that ensures $y^+=0.8$

In Table 5 results are presented. As can be observed in Table 5, changing the RANS model, there was no improvement in the prediction of the Nusselt number, so the k-ω-SST with a mesh that ensures $y^+=1$ has been chosen as future RANS model to apply when Reynolds numbers are higher than 5000, knowing that if Reynolds are lower than 5000, agreement with analytical and experimental results is poor.

Table 3. Comparison between pressure drops. Values obtained from numerical results have been compared to values obtained analytically by means of Kakac-Shah's and PKN correlation.

Re	e% f_{CFD} vs $f_{Kakac-Shah}$	e% f_{CFD} vs f_{PKN}
2168	19%	27%
3249	11%	19%
5399	3%	11%
7552	1%	8%

Table 4. Comparison between Nusselt numbers. Values obtained from numerical results have been compared to values obtained analytically by means of Gnielinski correlation.

Re	e% $Nu_{m,CFD}$ vs $Nu_{Experimental}$	$Nu_{l,Gn}$	$Nu_{l,CFD}$	e% $Nu_{l,CFD}$ vs $Nu_{l,Gn}$	$Nu_{m,Gn}$	$Nu_{m,CFD}$	e% $Nu_{m,CFD}$ vs $Nu_{m,Gn}$
2168	32%	6.67	10.83	62%	7.24	11.53	59%
3249	41%	10.97	14.17	29%	11.90	14.94	26%
5399	7%	17.88	20.26	13%	19.40	21.12	9%
7552	8%	23.81	25.91	9%	25.84	26.80	4%

4. Conclusion

In this paper the CFD model built for a high aspect ratio rectangular channel is presented. Agreement with analytic solution is good both at fluid-dynamic and thermal level with increasing error at low Reynolds numbers regarding turbulent flows.

Boundary conditions suitable to represent numerically the experimental set-up have been found. Regarding the most suitable RANS model, the k-ω-SST has been chosen as future RANS model to apply when Reynolds numbers are higher than 5000 to obtain acceptable numerical results.

The mesh needs to ensure $y^+=1$ near walls and no further thickness of the mesh is required. For low Reynolds number, there is thought to be no room for improvement using RANS models.

This model has been built as a starting point to be able to subsequently expand the thermo-fluid dynamics study of high aspect ratio channels even in the presence of ribbed surfaces considering flows operating at Reynolds number higher than 5000.

Table 5. Comparison between Nusselt numbers obtained from different CFD simulations with analytical and experimental values of Nusselt numbers. Reynolds number considered for this comparison has been equal to 3249.

RANS model tested	e% $Nu_{l,CFD}$ vs $Nu_{l,Gn}$	e% $Nu_{m,CFD}$ vs $Nu_{m,Gn}$	e% $Nu_{m,CFD}$ vs $Nu_{Experimental}$
k-ω-SST with y^+=1	29%	26%	41%
k-ω-SST with y^+=0.8	30%	26%	41%
k-ω-SST with y^+=0.2	30%	26%	42%
k-ω-SST with y^+=1 and Low Reynolds	56%	48%	66%
k-ε RNG with y^+=0.8	52%	45%	63%
k-ε Realizable y^+=0.8	43%	37%	54%

Nomenclature

Symbol	Quantity	SI Unit
A	Area	m^2
a	Channel half width	m
b	Channel half height	m
D_h	Equivalent diameter	m
f	Friction factor	-
h	Convective heat transfer coefficient	W/m^2K
k	Thermal conductivity	W/m/K
k	Turbulent kinetic energy	m^2/s^2
L	Channel length	m
ṁ	Mass flow rate	kg/s
Nu	Nusselt number	-
P	Pressure	Pa
Re	Reynolds number	-
T_b	Bulk temperature	K
T	Temperature	K
u_m	Bulk velocity (average)	m/s
q̇	Wall heat flux	W/m^2
$x_{fd,h}$	Hydrodynamic entry length	m
$x_{fd,th}$	Thermal entry length	m
y+	Dimensionless wall distance $y^+ = \Delta_{y_P}/\nu \sqrt{\tau_w/\rho}$	-
α^*	Aspect ratio	-
ν	Kinematic viscosity	m^2/s

ρ	Density	kg/m³
τ_w	Wall shear stress	Pa
ω	Specific dissipation rate	1/s

Subscripts

Symbol	Quantity
in	Inlet
l	Local, at a defined position
ln	Logarithmic
m	Mean
out	Outlet
w	Wall
z	Local, at a position that varies with z
∞	Free stream, at ∞ location

References

[1]   Webb R L, and Kim N H, (2004). Principles of Enhanced Heat Transfer (2nd ed.). Garland Science. https://doi.org/10.1201/b12413

[2]   Nourin F N, and Amano R S, Review of Gas Turbine Internal Cooling ImprovementTechnology, J. Energy Resour. Technol. Trans. ASME, vol. 143, no. 8, pp. 1–8, 2021, 10.1115/1.4048865

[3]   D Fustinoni et al 2012 J. Phys.: Conf. Ser. 395 012042, 10.1088/1742-6596/395/1/012042

[4]   D Fustinoni et al 2015 J. Phys.: Conf. Ser. 655 012060, 10.1088/1742-6596/655/1/012060

[5]   D Fustinoni et al 2017 J. Phys.: Conf. Ser. 796 012015, 10.1088/1742-6596/796/1/012015

[6]   Niro A, Gramazio P, Vitali L and Fustinoni D, Local and global heat transfer characteristics inside a rectangular channel of 1:10 aspect-ratio with ribbed surfaces, International Heat Transfer Conference, pp. 5509-5516, 2018, 10.1615/IHTC16.hte.023149

[7]   Sharma S K and Kalamkar V R, Computational Fluid Dynamics approach in thermo-hydraulic analysis of flow in ducts with rib roughened walls - A review, vol. 55. Elsevier, 2016, 10.1016/j.rser.2015.10.160

[8]   Kakaç S, Shah R K and Aung W. Handbook of Single-Phase Convective Heat Transfer. New York: Wiley, 1987. Print. (Ch. 3-4)

[9]   Shah R K and London A L, Laminar Flow Forced Convection in Ducts: A Source Book for Compact Heat Exchanger Analytical Data, vol. Suppl. 1. Academic Press, 1978

[10]   Techo R, Tickner R R and James E, (June 1, 1965). An Accurate Equation for the Computation of the Friction Factor for Smooth Pipes From the Reynolds Number. ASME. J. Appl. Mech. June 1965; 32(2): 443, 10.1115/1.3625826

[11]   Prandtl L, Führer durch die Strömungslehre, Braunschweig (1944). English Version Transl., Blackie, London 1952

[12]   T. von Karman, Turbulence and Skin Friction, J. Aerops. Sci., Vol. 7, pp. 1-20, 1934, https://doi.org/10.2514/8.5

[13]   Nikuradse J, Laws of Turbulent Pipe Flow in Smooth Pipes (1933), English transl., NACA TT F-10, 359, 1966,

[14]   Bergman T L, Lavine A S, Incropera F P, and Dewitt D P, Fundamentals of Heat and Mass Transfer. John Wiley & Sons, 2011. (Ch. 8-11)